Electronic Supplementary Material (ESI) for Reaction Chemistry & Engineering.
This journal is © The Royal Society of Chemistry 2023

Electronic Supporting Information

Design and evaluation of a microrectification platform using 3D printing

Yuting Zheng, Guandong Fang, Zhuoqin Fan, Haomiao Zhang*, Jingdai Wang, Yongrong Yang

State Key Laboratory of Chemical Engineering, College of Chemical and Biological Engineering, Zhejiang University, 310058, P.R. China
E-mail: haomiaozhang@zju.edu.cn

S1. Materials and chemicals

S1.1 3D printing materials

A High Temp Resin (FLFLGR02) with a print resolution of 25 μm was purchased from Formlabs and used in this study. Formlabs measured resistance of this resin to solvents by observing, measuring, and weighing cured resin cubes (originally measuring 1 cm × 1 cm × 1 cm) before and after soaking in a solvent for 24 hours.[1] We further measured several solvents following the same procedure. All the results are summarized in Table S1, indicating sufficient chemical compatibility under exposure to n-hexane and cyclohexane.

Table S1. Weight gain (%) by resin "FLFLGR02" after 24-hour exposure to solvents.

Solvent	Weight gain [%]	Reference
n-Hexane	< 1	This work
Cyclohexane	< 1	This work
Toluene	Cracked	This work
Acetone	< 1	[1]
Isopropyl Alcohol	< 1	[1]
Hydrogen peroxide (3%)	< 1	[1]
Salt Water (3.5% NaCl)	< 1	[1]
Strong acid (HCl conc)	1.2	[1]
Sodium hydroxide (0.025%, pH 10)	< 1	[1]

S1.2 Rectification experiments

Cyclohexane (99.5%) and n-Hexane (97.0%) were obtained from Aladdin Chemical Co., Ltd. Both chemicals were used as received.

S2. Experimental

S2.1 Experimental apparatus

Fig. S1 shows a photo of the experimental apparatus, which primarily encompasses a plunger pump for the feed, two peristaltic pumps to control the reflux and reboiling ratios, an oil bath (reboiler), an ice bath (condenser), and a 3D printed microrectification column wrapped by an insulation tape.

Fig. S1 Photo of the experimental apparatus.

S2.2 Tray column structures

In this work, we design four different rectification columns; three of them are tray columns (i.e., Helix, Sieve, and Weir), and the other one is a packed column with sphere packings (i.e., Sphere). Table S2 summerize the detailed column information, in which L_e is the effective column length (length of the tray/packed structure), and L_c is the characteristic length used for Bo number calculation. L_c is determined by the smallest feasure of the structure.

Table S2. Comparison of the detailed column information

Column Type	Structure	L_e, m	Volume, m^3	Porosity, %	L_c, μm	Bo
Tray	Helix	0.082	8.92×10^{-6}	70.8	500	0.0959
Tray	Sieve	0.082	1.08×10^{-5}	85.7	700	0.188
Tray	Weir	0.093	1.14×10^{-5}	79.7	400	0.0614

Packed	Sphere	0.082	5.57×10^{-6}	44.2	300	0.0345

S2.2.1 Helix

The Helix structure is based on a coiled channel with a diameter of 6.6 mm, and multiple straight channels of diameter 0.5 mm. By design, the liquid phase travels down along the coiled channel while the vapor rises through the straight channels (Fig. 2a-b). The vapor and liquid are mixed in the intersection of channels. The smallest feature in this design is 0.5 mm. Fig. S2 presents the detailed dimensions of this structure.

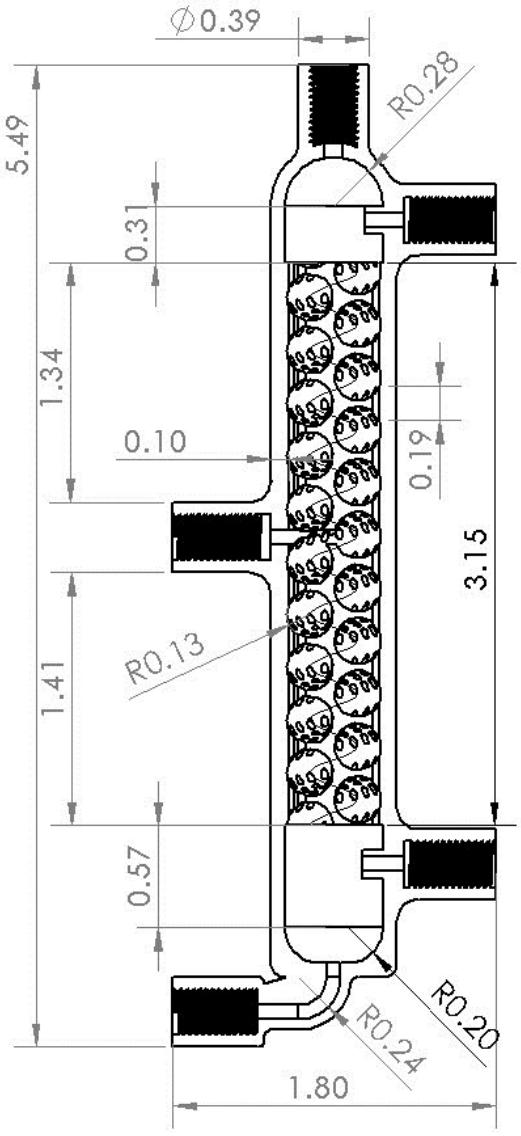

Fig. S2 Detailed dimensions of the Helix structure in inches.

S2.2.2 Sieve

The Sieve column is designed based on a simple perforated sieve plate with the smallest feature of 0.7 mm (see Fig. 2c-d). A rotation angle of 90 degrees exists between any two adjacent plates. The distance between any two adjacent plate is 3.05 mm. Fig. S3 presents the detailed dimensions of this structure.

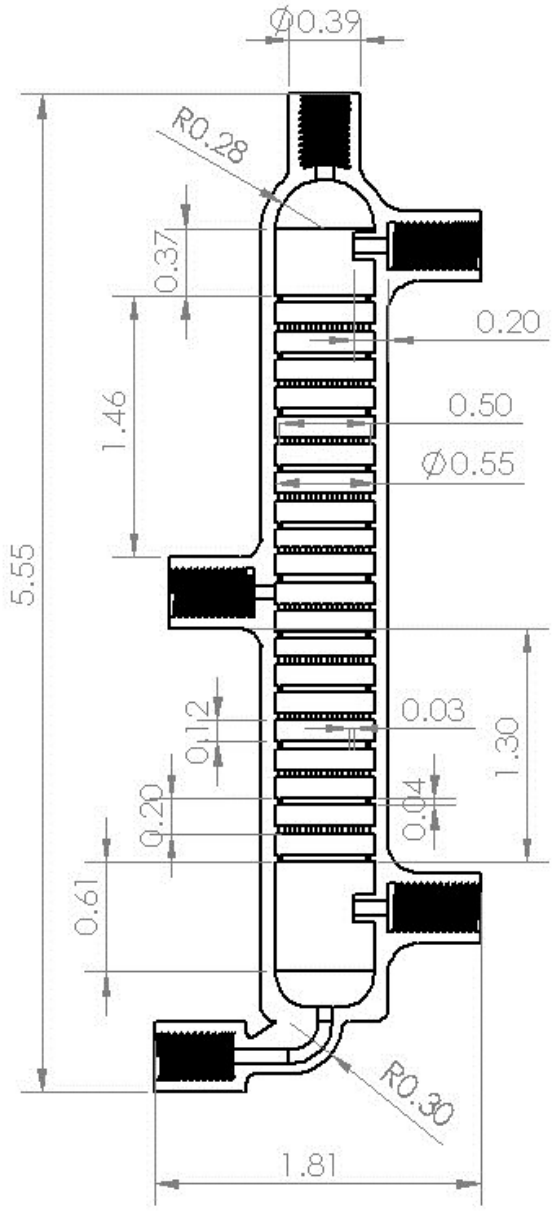

Fig. S3 Detailed dimensions of the Sieve structure in inches.

S2.2.3 Weir

The Weir structure is more likely a miniature version of a conventional tray column featured with overflow weirs, in which plates with holes are rotated and stacked together (see Fig. 2e-f). The diameter of the holes on the tray, as the smallest feature, is 0.4 mm. The distance between any two adjacent plate is 5.08 mm. Fig. S4 presents the detailed dimensions of this structure.

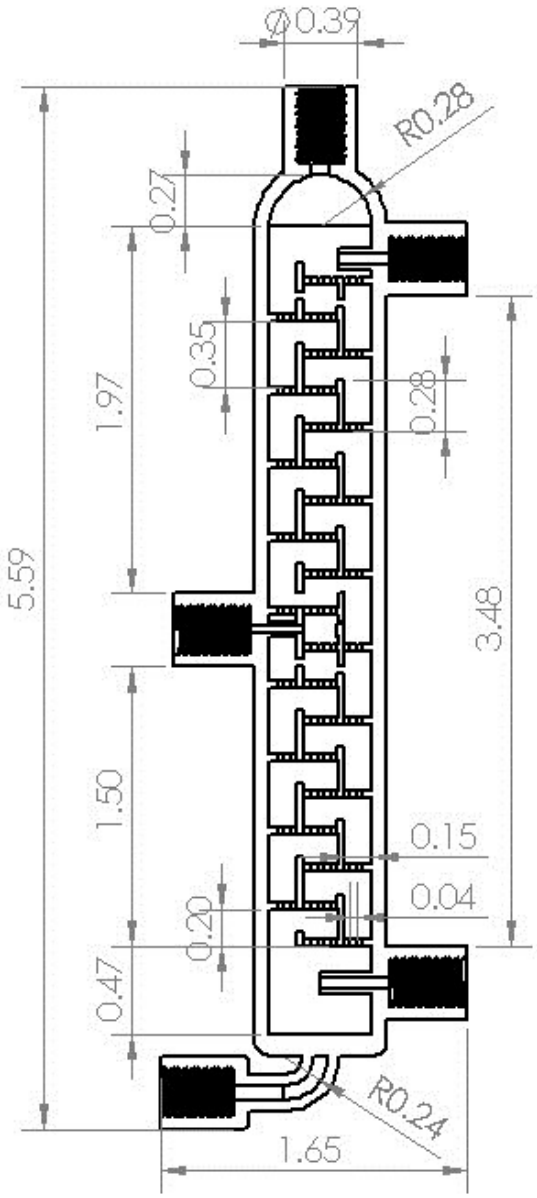

Fig. S4 Detailed dimensions of the Weir structure in inches.

S2.2.4 Top and bottom structures

The 3D structures of the top and bottom regions are illustrated in Fig. S5. The top region has one inlet and one outlet for the reflux stream; similarly, the bottom region has one inlet and one outlet for the reboiling stream.

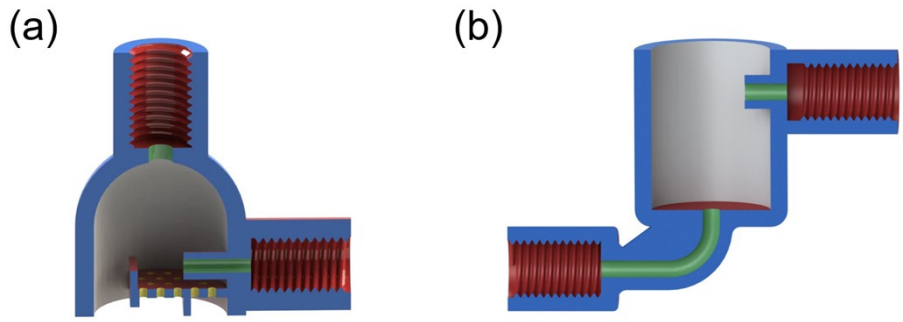

Fig. S5 Structure of (a) the top and (b) the bottom sections.

S2.3 Inline mixers for boiling in microchannels

The connecting tubing immersed in the oil bath (100 ^{o}C) has an inner diameter of 1.59 mm and an outer diameter of 3.18 mm. Controlling liquid boiling in such small channels is challenging due to the reduced nucleation, as surface effects play an important role during flow boiling in microchannels. In the absence of dissolved gas or surface nucleation sites, liquid is easily superheated during flow without boiling. In order to prevent the formation of superheated liquid mixtures, we employ an in-house designed and 3D printed spring-type inline mixer (see Fig. S6 for the structure) as well as sphere ceramic packings (mean diameter 1 mm) in the connecting tubing to generate nucleation. Visible boiling is therefore observed on the surface of the mixer/packings.

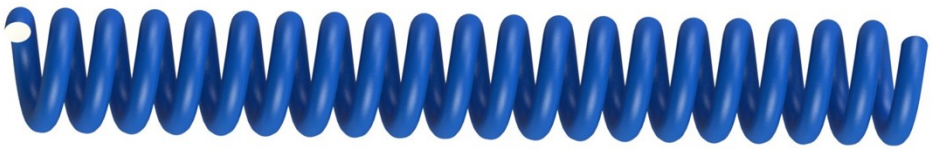

Fig. S6 Structure of the inline mixer. The length is 10 mm and the diameter of the spring is 300 μm. This structure is defined by Pitch and Revolution in SOLIDWORKS, with the Pitch setting of 0.50 mm and Revolutions of 20.

S3. Mass transfer model

S3.1 Model description

The steady state mass conservation equation of the rectification column is eqn(S1). With the assumption of one dimension, this equation reduces to eqn(10).

$$\nabla \cdot j_i + \rho(u \cdot \nabla)\omega_i = R_{i,k} \qquad (S1)$$

We use the mixture-averaged approximation of the multicomponent diffusion model, which assumes the mass flux due to molecular diffusion is determined by a Fick's law type expression. The mass flux (j_i) and the mixture averaged diffusion coefficients (D_i^m) are presented in eqn(S2)-(S3), where ρ_i and x_i are the density and mole fraction of species i, and the Maxwell-Stefan diffusion coefficient D_{ik} is replaced with the binary diffusivities. In addition, thermal diffusion is ignored in the model.

$$j_i = -\rho_i D_i^m \frac{\nabla x_i}{x_i} \qquad (S2)$$

$$D_i^m = \frac{1-\omega_i}{\sum_{k \neq i}^{N} \frac{x_k}{D_{ik}}} \qquad (S3)$$

For the liquid phase, the boundary conditions used are eqn(S4)-(S6),

At top (distillate): $x^L = x_D$ $(S4)$

In the feed: $x^L = x_F$ $(S5)$

At bottom (bottom product): $j^L = 0$ $(S6)$

For the vapor phase, the boundary conditions used are eqn(S7)-(S8),

At top (distillate): $j^V = 0$ $(S7)$

At bottom (bottom product): $x^V = x_B$ $(S8)$

S3.2 Computer information

All simulations are performed on a ThinkPad P50 Workstation with Intel Core i7-6820HQ CPU @ 2.70GHz and 64GB RAM.

S4. Literature reported HETP in microrectification columns

Table S3 presents the dimension (D, i.e., diameter or length x width) and HETP of the literature reported microdistillation/microrectification columns.

Table S3. Comparison of similar microdistillation/microrectification columns.

Structure	D, mm	HETP, cm	Separated mixture	Reference
Micro wick	Φ10.5	5-7	EtOH/H_2O, MeOH/H_2O	[2]
Metal foam	30×5	5	$HCOOCH_3$/MeOH	[3]
Micro channel	0.5×1	1.56	$^{10}BF_3$/$^{11}BF_3$	[4]
Tray	35×5	1.08	toluene/n-octane	[5]
Packing	Φ7	8.8	n-hexane/cyclohexane	[6]
Spinning-band	Φ50	5-8	EtOH/MeOH	[7]

Reference

[1]https://formlabs-media.formlabs.com/filer_public/ac/89/ac8963db-f54a-4cac-8fe9-fb740a7b06f1/formlabs-materials-library.pdf

[2] Seok D R, Hwang S T. Zero-gravity distillation utilizing the heat pipe principle(micro-distillation), AIChE Journal, 1985, 31(12): 2059-2065.

[3] Sundberg A T, Uusi-Kyyny P, Jakobsson K, et al. Control of reflux and reboil flow rates for milli and micro distillation, Chemical Engineering Research and Design, 2013, 91(5): 753-760.

[4] Tang Y, Zheng Y J, Tian J Z, et al. Process intensification of chemical exchange method for boron isotope separation using micro-channel distillation technology, Micromachines, 2021, 12(10): 1222.

[5] Ziogas A, Cominos V, Kolb G, et al. Development of a microrectification apparatus for analytical and preparative applications, Chemical Engineering & Technology, 2012, 35(1): 58-71.

[6] Mardani S, Ojala L S, Uusi-Kyyny P, et al. Development of a unique modular distillation column using 3D printing, Chemical Engineering and Processing - Process Intensification, 2016, 109: 136-148.

[7] Bittorf L, Böttger N, Neumann D, et al. Characterization of an automated spinning-band column as a module for laboratory distillation, Chemical Engineering & Technology, 2021, 44(9): 1660-1667.